3D Printing of High-Strength Water-Soluble Salt Cores Via Layered Extrusion Forming

Xiaolong Gong (gongxl@hust.edu.cn)
Huazhong University of Science and Technology School of Material Science and Engineering
Xinwang Liu
Huazhong University of Science and Technology School of Material Science and Engineering
Zheng Chen
Huazhong University of Science and Technology School of Material Science and Engineering
Zhiyuan Yang
Huazhong University of Science and Technology School of Material Science and Engineering
Wenming Jiang
Huazhong University of Science and Technology School of Material Science and Engineering
Zitian Fan
Huazhong University of Science and Technology School of Material Science and Engineering

Research Article

Keywords: Additive manufacturing, layered extrusion forming, water-soluble salt cores, bauxite powder, reinforcement

Posted Date: May 27th, 2021

DOI: https://doi.org/10.21203/rs.3.rs-546973/v1

3D printing of high-strength water-soluble salt cores via layered extrusion forming

Xiaolong Gong, Xinwang Liu*, Zheng Chen, Zhiyuan Yang, Wenming Jiang, Zitian Fan*

State Key Laboratory of Materials Processing and Die & Mould Technology, School of Materials Science and Engineering, Huazhong University of Science and Technology, Wuhan 430074, China

Abstract: Core materials with high strength and excellent collapsibility are important for the manufacture of hollow composite structure castings. In this work, a novel technology to fabricate water-soluble Na_2SO_4-NaCl based salt cores with high strength and low cost by layered extrusion forming (LEF) was reported. The water-soluble Na_2SO_4 and NaCl powder were used as the matrix materials, and the bauxite powder was used as the reinforcing material. The effects of bauxite powder content and liquid phase sintering parameters on properties of the salt cores were studied. The results show that the salt-based slurry exhibits shear thinning property within the studied bauxite powder contents. When the content of bauxite powder was 20 wt.% and the sintering was at 630 ℃/30 min, the obtained salt cores show an optimal comprehensive performance, with the bending strength, linear shrinkage, water-solubility rate and moisture rate of 24.43 MPa, 6.3%, 207.6 (g/min·m^2), and 0.29%, respectively. The complex water-soluble salt core samples prepared under the optimal parameters display high-strength and well-shaped morphology.

Keywords: Additive manufacturing; layered extrusion forming; water-soluble salt cores; bauxite powder; reinforcement.

1 Introduction

With the rapid development of aerospace, automotive and communications industries, light alloy castings, such as aluminum, magnesium alloy die castings, have been widely used in these fields [1-3]. However, in order to further pursue the structural

* Corresponding authors:

E-mail addresses: liuxw@hust.edu.cn (X. Liu), fanzt@hust.edu.cn (Z. Fan)

rationality and lightweight of the key parts, the light alloy die castings tend to be integrated and complicated, resulting in more complex internal cavity channels inside the castings, which put forwards higher requirements for the core materials used to form complex hollow-structure castings [4-6]. Normally, the sand cores cannot meet the conditions of industrial applications due to their lower strength and poor collapsibility, while the ceramic cores have poor collapsibility in spite of sufficient strength [7-11].

The water-soluble salt cores have attracted considerable attention due to their excellent properties including high strength, low gas evolution and good water-soluble collapsibility, which are desired for the preparation of complex hollow composite structures castings [12-15]. Liu and Gong et al. [16,17] prepared KNO_3-based water-soluble salt cores with bending strength of 42-46 MPa for zinc alloy die castings by gravity casting method. Yaokawa et al. [13] fabricated salt cores composed of alkali carbonate and alkali chloride with bending strength of 20-30 MPa for aluminum alloy die castings by gravity casting method. Jelínek et al. [18] reported NaCl and KCl salt cores with bending strength of 5.3-10 MPa through squeezing technology using alkali silicates as a binder. Sakoda et al. [19] prepared NaCl and KCl salt cores with bending strength of 20-37 MPa for aluminum alloy die castings by pressing sintering method. Among all these researches, the bending strength of the salt cores fabricated by gravity casting method or pressing sintering method had exceeded 20 MPa, which can be used for the manufacture of aluminum alloy die castings. However, these traditional methods have some disadvantages, such as necessary molds, high cost, high energy consumption, et al. Especially, the geometric design and structural complexity of salt core products are limited by the current forming processes, which seriously impedes its industrial application. Therefore, it is of great significance to explore a new forming process to prepare complex water-soluble salt cores with high strength and low cost.

Layered extrusion forming (LEF), as a kind of additive manufacturing technology, can freely form parts without molds [20,21], which provides a new direction for the preparation of complex water-soluble salt cores with a low cost. In the LEF technology, the solid powder materials are made into a uniformly dispersed slurry, and then the slurry is continuously extruded to form components under certain pressures according

to the designed geometry [22,23]. In recent years, this technology has been used to prepare high-porosity structural parts and biomedical scaffolds with NaCl, $CaCl_2$, and $CuSO_4$ as the matrixes [24-26]. Due to the excellent water solubility of inorganic salt materials, all these studies have focused on the spatial network structure, but ignoring improving the mechanical properties of the salt-based templates. The salt cores materials and sintering process are critical to the mechanical properties of the water-soluble salt core. However, there are few reports on the preparation of high-strength water-soluble salt cores through the LEF method.

In this paper, a novel method was developed to fabricate high-strength salt cores by layered extrusion forming using Na_2SO_4 powder and NaCl powder as the matrix material, and the bauxite powder was selected as the reinforcing material. The effects of bauxite powder content and liquid phase sintering parameters on the bending strength, linear shrinkage, water-solubility, porosity of the salt cores were investigated. The optimized process parameters were obtained. Finally, the complex water-soluble salt core components with high strength were prepared under optimized experimental conditions. This method provides a new way to obtain complex water-soluble salt cores with high strength and low cost, which has important theoretical and practical significance for the water-soluble salt cores in industrial development.

2 Materials and methods

2.1 Raw materials

In this study, water-soluble sodium sulfate powder (Na_2SO_4, 95 wt.% purity, D_{50}=12.5 μm) and sodium chloride powder (NaCl, 99 wt.% purity, D_{50}=75 μm) were selected as the matrix materials. Bauxite powder (D_{50}=45 μm, Zhengzhou Xiangyu Casting Material Co., Ltd., China) was selected as the reinforcing material. Anhydrous ethanol (EtOH, Analytical purity, Sinopharm Chemical Reagent Co., Ltd., China) was adopted as a carrier liquid for preparing the salt-based slurry. Polyvinyl pyrrolidone (PVP, Shandong Yousuo Chemical Technology Co., Ltd., China) was used as a binder, and methyl silicone oil was used as a release agent. The compositions of the salt-based slurry are listed in Table 1, and the mole percentage of Na_2SO_4 and NaCl is 30 mol%:70

mol%.

Table 1 Compositions of the salt-based slurry.

Liquid component		Solid powder			Proportion of bauxite
EtOH (g)	PVP (g)	Na_2SO_4 (g)	NaCl (g)	Bauxite (g)	in solid powder (wt.%)
20.4	3.6	38.75	37.25	0	0
		36.81	35.39	3.8	5
		34.88	33.52	7.6	10
		31.0	29.80	15.2	20
		27.13	26.07	22.8	30

2.2 Preparation process

Fig. 1 depicts the schematic diagram of preparing water-soluble salt cores via LEF technology. The preparation process of the salt cores mainly includes salt-based slurry preparation, extrusion forming and sintering. The solid powder (Na_2SO_4, NaCl and bauxite) was first added to an anhydrous ethanol solution with 15 wt.% PVP and stirred manually, and then ball milling was carried out in a planetary mixer for 8 h at 180 rpm to obtain a stable salt-based slurry. To follow, the salt-based slurry was transferred to a layered extrusion device made by our research group. The salt-based slurry was extruded according to the designed route by pneumatic actuation to form the required samples at room temperature, and the printing parameters of the LEF technology are shown in Table 2. Finally, the salt core green body was dried in drying oven at 50 ℃ for 8 h, and the dried green body was sintered at the set temperature to obtain salt core samples.

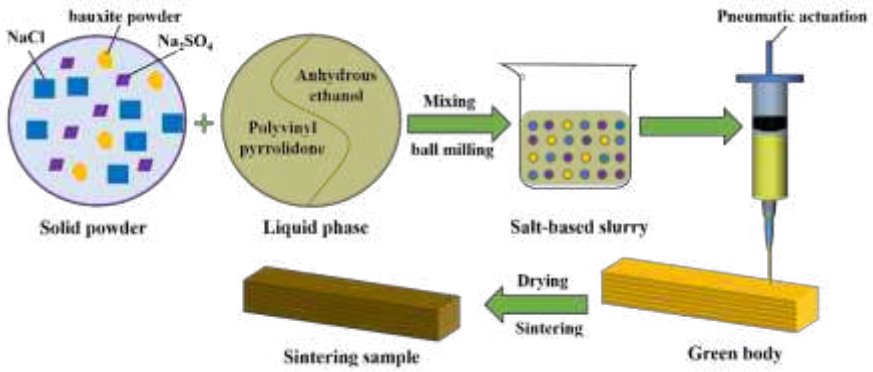

Fig.1 Schematic diagram of the LEF technology to prepare water-soluble salt cores.

Table 2 Printing parameters for salt-based slurry.

Printing parameters	Values
Nozzle diameter	0.41 mm
Layer height	0.38 mm
Printing speed	20 mm/s
Air pressure	0-2 kg/cm^2

2.3 Measurement and Characterization

A stress-controlled rheometer (DHR-2, TA, USA) was used to test the rheological behaviors of the salt-based slurry with a parallel plate of 25 mm in diameter and a testing gap of 1000 μm. An ElectroPuls all-electric dynamic and fatigue test systems (ElectroPuls E1000, Instron, USA) was used to measure the bending strength of the salt cores using a three-point-bending method with a span of 30 mm and a pressure head loading speed of 0.5 mm/min, and five samples (50 × 7 × 7 mm in length, width, and height, respectively) were measured in each group to reduce the error. The water-solubility rate (K) of the salt cores was calculated by Eq. (1).

$$K = \frac{m}{s \times t} \quad (1)$$

Where m and s represent the mass and total surface area of the salt core samples, respectively, t is the dissolution time of the salt core samples in still water at 40 ℃. The linear shrinkage (L) of the salt core samples was measured according to Eq. (2).

$$L = \frac{l_1 - l_2}{l_1} \times 100\% \quad (2)$$

Where l_1 and l_2 represent the length of dried samples and sintered samples, respectively. The moisture rate (φ) of the salt core samples was calculated according to Eq. (3).

$$\varphi = \frac{m_1 - m_0}{m_0} \times 100\% \quad (3)$$

Where m_0 represents the original mass of the salt core samples, and m_1 represents the mass of the salt core samples exposed to the air (relative humidity: 60%-70%) for 2 days. The bulk density (D_b), open porosity (P_o) and closed porosity (P_c) of the salt core samples were tested using the Archimedes method with the equations respectively displayed in Eqs. (4) and (5) [27]:

$$P_o = \frac{M_1 - M_0}{M_1 - M_2} \times 100\% \quad (4)$$

$$P_c = \frac{M_0 - M_2 - M_o \times \rho_0/\rho_r}{M_1 - M_2} \times 100\% \quad (5)$$

Where M_0 represents the mass of dried salt core samples, M_1 is the mass of kerosene-saturated salt core samples in air, and M_2 is the mass of samples in kerosene. ρ_0 is the density of kerosene (0.8 g/cm^3), and ρ_r is the real density of the salt core samples.

Thermogravimetric and differential thermal analysis (TG-DTA, PerkinElmer Instruments) were performed on the green body after drying to determine the sintering process, and the heating temperature was increased from room temperature to 640 ° C at a rate of 10 ° C/min. The compositions of the salt core samples were analyzed using X-ray diffraction (XRD-7000S, Japan) with a Cu Kα radiation. The micromorphology of the salt core samples pretreated by carbon sputtering was observed using a scanning electron microscope (SEM, Quanta 200) equipped with an energy dispersive spectrometer (EDS).

3 Results and discussion

3.1 Layered extrusion forming of salt cores

Rheological properties of the salt-based slurry are critical to fabricate the salt cores using a LEF method, and the rheological behaviors of salt-based slurry with different bauxite powder contents are shown in Fig. 2. It can be observed that the salt-based

slurry with different bauxite powder contents exhibits shear thinning property, which means that the salt-based slurry can be extruded smoothly from the nozzle, and the extruded slurry will be rapidly deposited and formed without shear force. Meanwhile, it can also be seen that the viscosity and shear stress of the slurry decrease as the content of bauxite powder increases. The reason is that the density of bauxite powder (3.45 g/cm^3) is greater than that of NaCl (2.16 g/cm^3) and Na_2SO_4 (2.68 g/cm^3). increasing of bauxite powder content, the volume fraction of the solid powder (Na_2SO_4, NaCl and bauxite) decreases, leading to the decrease of the solid content of the salt-based slurry.

The salt core green body prepared by LEF technology was then sintered in order to obtain excellent mechanical property. The sintering process of the salt core green body was determined by the TG-DTA results, as shown in Fig. 3. It can be seen from Fig. 3(a) that the PVP in salt core green body is decomposed at about 350 ℃, and with the further increase of temperature, the salt core green body begins to melt at about 620 ℃, which is in good agreement with the solidus temperature of NaCl-Na_2CO_3 binary phase diagram [28]. The liquid phase sintering temperature was set to 630℃ based on our previous experiments. Therefore, the sintering process of the salt core green body was carried out according to Fig. 3(b). First, the salt core green body was calcined at 350 ℃ for 1 h with a heating rate of 1 ℃/min to remove the PVP organic matter, and then elevated the temperature to 600 ℃ at a heating rate of 3 ℃/min, and the temperature was kept for 60 min to ensure the same temperature inside and outside the salt cores. Finally, it was heated to 630 ℃ and kept for 15 min, 30 min and 45 min respectively to complete the liquid phase sintering and obtain the salt core samples.

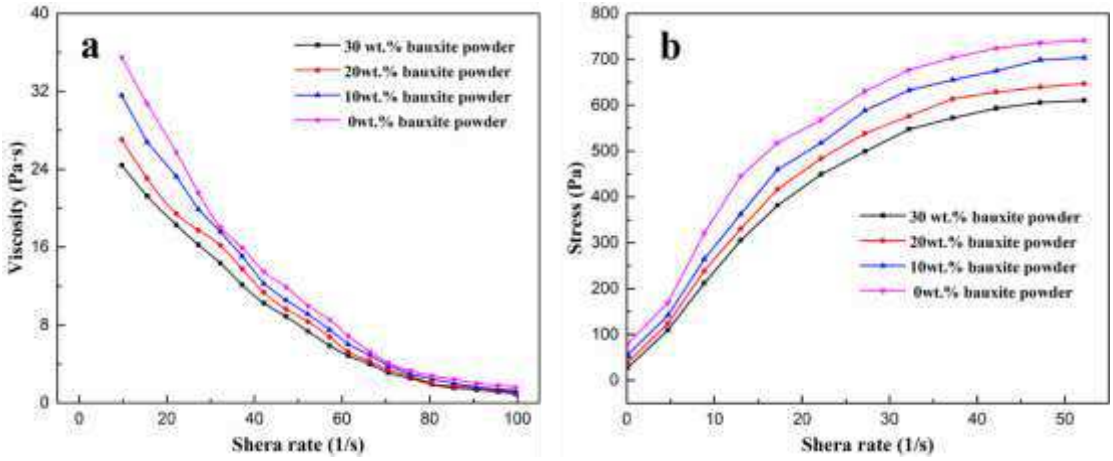

Fig. 2 Rheological behaviors of salt-based slurry with different bauxite powder contents: (a) viscosity versus shear rate and (b) stress versus shear rate.

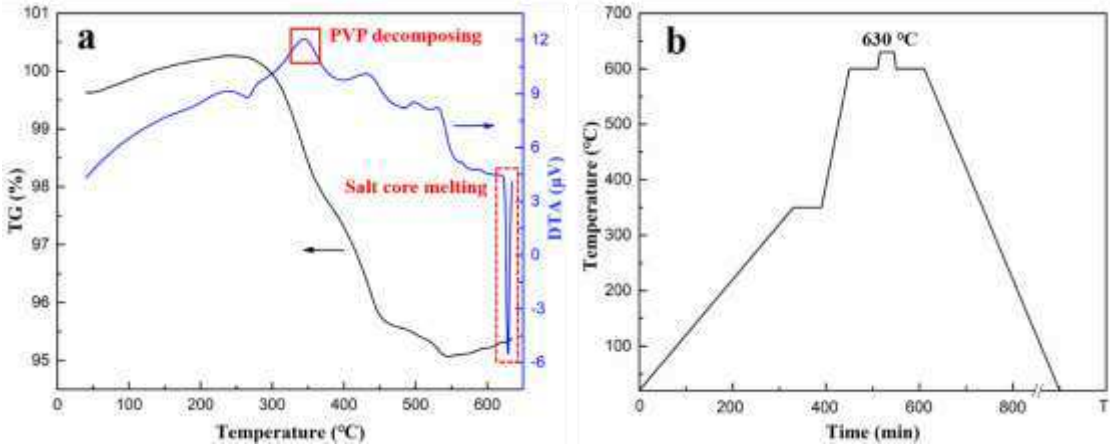

Fig. 3 Sintering process of salt core green body: (a) TG-DTA curves and (b) sintering temperature versus sintering time.

3.2 Performance characteristics

Fig. 4 shows the effects of bauxite powder content at various sintering time on bending strength and linear shrinkage of the salt core samples. It is evident that the bauxite powder content and sintering time have a remarkable influence on the bending strength and linear shrinkage of the salt core. As illustrated in Fig 4(a), when the sintering time is 15 min, the bending strength of the salt core is less than 9 MPa, and the bending strength decreases with the increase of bauxite powder content. When the sintering time is 30 min and 45 min respectively, the bending strength of the salt core increases first and then decreases as the content of bauxite powder increases. For example, when the sintering time is 30 min, the bending strength of the salt core increases dramatically from 14.56 MPa to 24.43 MPa with increasing the bauxite powder content from 0 wt.% to 20 wt.%, and then decreases to 18.68 MPa as the bauxite powder content further increase to 30 wt.%. It should be noted that the salt core samples without bauxite powder (0 wt.%) are destroyed by excessive melting when the sintering time is 45 min.

As illustrated in Fig 4(b), when the sintering time is constant, the linear shrinkage of the salt core decreases with the increase of bauxite powder content. When the content of bauxite powder is constant, the linear shrinkage increases with the increase of

sintering time. For example, when the sintering time is 30 min, with the content of bauxite powder increasing from 0 wt.% to 30 wt.%, the linear shrinkage decreases from 10.5% to 4.2%. It is well known that the bending strength and linear shrinkage are the main properties of the salt core. First, the salt core is a brittle material and needs high strength to resist the impact of liquid metal during high pressure die casting. Secondly, low shrinkage is necessary to ensure the precision of castings.

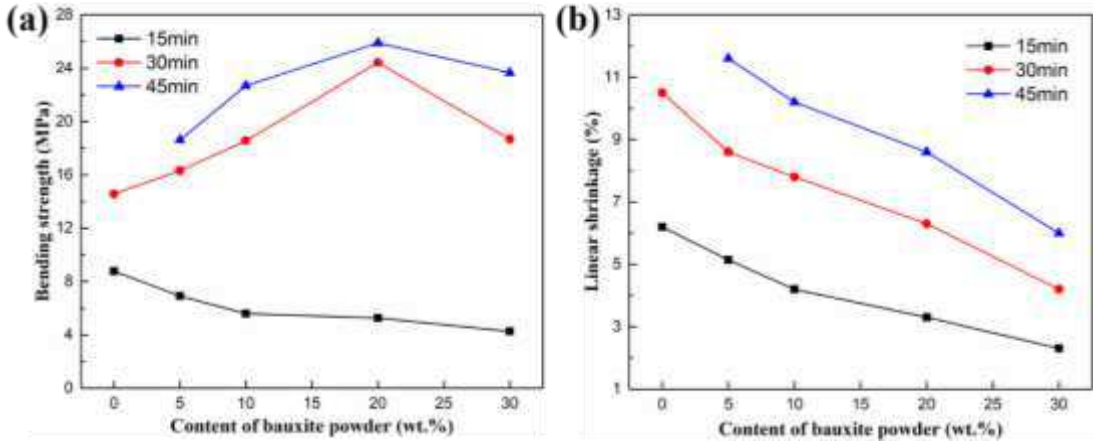

Fig. 4 Effects of bauxite powder content at various sintering time on the salt core samples: (a) bending strength and (b) linear shrinkage.

Fig. 5 shows the effects of bauxite powder content at various sintering time on open porosity and close porosity of the salt core samples. As can be seen, the open porosity decreases with the increase of sintering time, while the close porosity shows the opposite trend. When the content of bauxite powder is 20 wt.%, the open porosity decreases dramatically from 21.97% to 3.08% with increasing the sintering time from 15 min to 45 min, while the closed porosity increases from 4.5% to 9.58%. When the sintering time is 15 min, the salt core possesses a higher open porosity and a lower closed porosity, which is caused by insufficient sintering time. When the sintering time is 30 min and 45 min, respectively, the open porosity increases slowly and then sharply with the increase of bauxite powder content. Such phenomenon might result from two factors. On the one hand, the bauxite powder is a refractory material that will improve the thermal stability of the salt core. On the other hand, the excessive bauxite powder is prone to agglomeration and would reduce the fluidity of the liquid phase [29].

Fig. 6 depicts the effects of bauxite powder content at various sintering time on

water-solubility rate and moisture rate of the salt core samples. As shown in Fig.6, the water-solubility rate and the moisture rate display an overall trend of decreasing with the increase of sintering time and bauxite powder content, respectively. When the sintering time is 30 min, as the bauxite powder content increases from 0 wt.% to 30 wt.%, the water-solubility rate of the salt core decreases from 336.7 (g/min·m^2) to 152.6 (g/min·m^2), and the moisture rate decreases from 0.49% to 0.27%. When the content of bauxite powder is 20 wt.%, with the increases of sintering time from 15 min to 45 min, the water-solubility rate and the moisture rate of salt core decrease from 322.1 (g/min·m^2) to 205.4 (g/min·m^2) and from 0.42% to 0.28%, respectively. For the water-soluble salt core, the higher water-solubility rate is beneficial to the removal from the castings, and the lower moisture rate is conducive to the storage of the salt core. Generally, the higher densification degree of the salt core, the lower its water-solubility rate and moisture rate. Furthermore, the bauxite powder as an insoluble material can also reduce the water-solubility rate and moisture rate of the salt core.

In conclusion, when the sintering time and the bauxite powder content are 30 min and 20 wt.%, respectively, the obtained salt core samples possess excellent comprehensive properties, which the bending strength, linear shrinkage rate, water-solubility rate and moisture rate are 24.43 MPa, 6.3%, 207.6 (g/min·m^2), 0.29%, respectively.

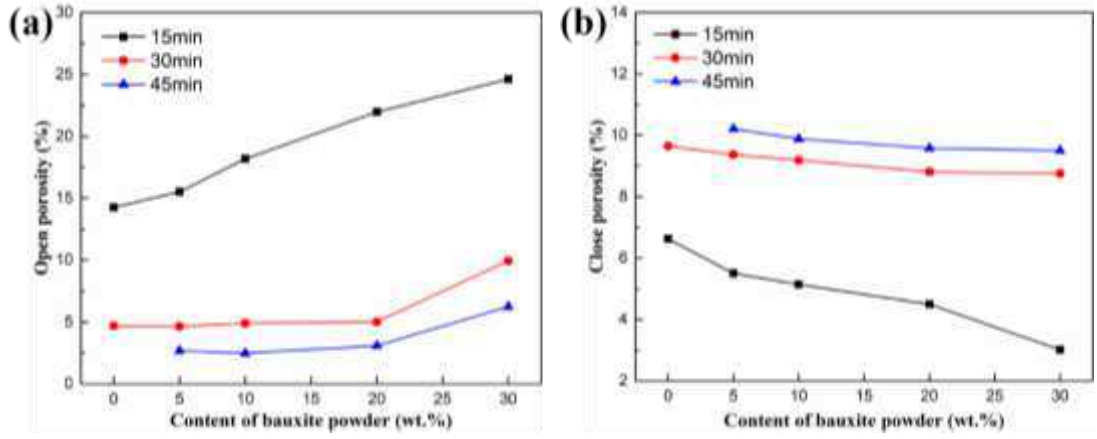

Fig. 5 Effects of bauxite powder content at various sintering time on the salt core samples: (a) open porosity and (b) close porosity.

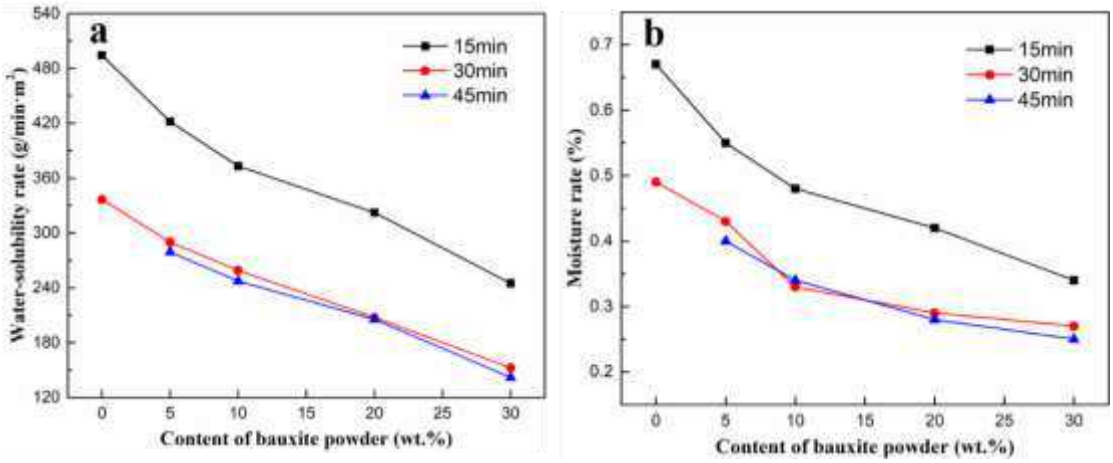

Fig. 6 Effects of bauxite powder content at various sintering time on the salt core samples: (a) water-solubility rate and (b) moisture rate.

3.3 Microstructure analysis

Fig. 7 shows the XRD patterns of the salt core samples with different bauxite powder contents sintered for 30 min. It can be observed that the salt cores are mainly composed of NaCl phase, Na_2SO_4 phase and Al_2O_3 phase, and there is no other new phase detected, which indicates that the bauxite powder has not reacted with the salt melt and stably exists in the salt core matrix.

Fig. 8 shows the EDS maps analyses of the salt core samples with 20 wt.% bauxite powder at 30 min sintering. It can be seen that the elements of Na, Cl, Al, S and O are clearly distributed in the salt core, and the NaCl (Cl element) and bauxite powder (Al element) are relatively dispersed in the salt core. Furthermore, it can also be observed that the bauxite powder is distributed around the NaCl phase.

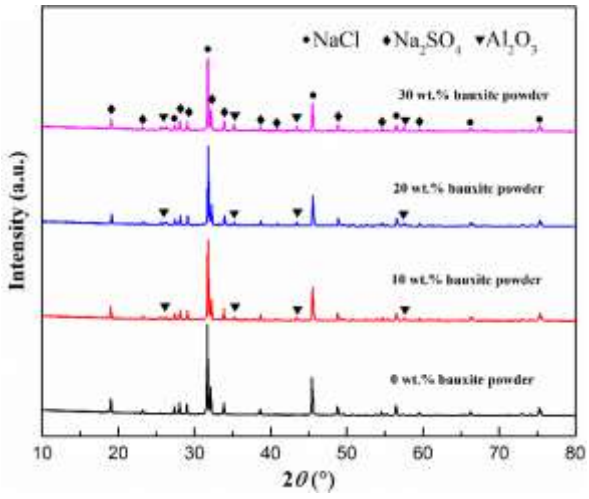

Fig. 7 XRD pattern of the salt core with different bauxite powder contents sintered for 30 min.

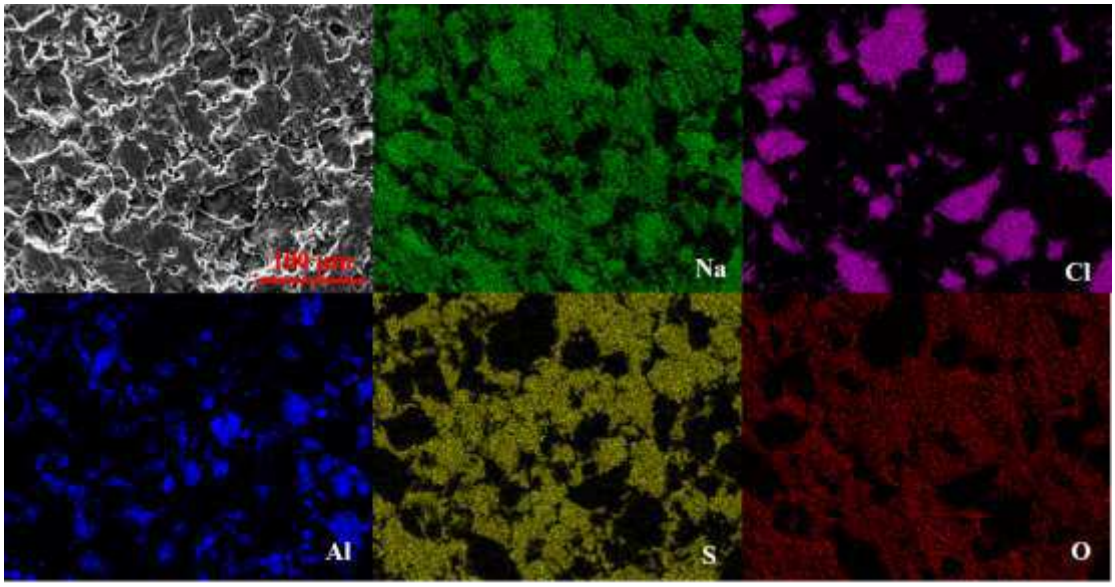

Fig. 8 EDS maps analyses of salt core samples with 20 wt.% bauxite powder sintered for 30 min.

Fig. 9 shows the microstructures of the salt core samples with 20 wt.% bauxite powder at different sintering time. When the sintering time is 15 min, as shown in Fig. 9(a) and (d), a large number of open pores are visible, and only a small amount of solid powder was sintered into agglomerates. When the sintering time is 30 min, as shown in Fig. 9(b) and (e), the pores of the salt core remarkably reduces and the densification degree increases. In addition, some closed pores are observed in the salt core. As the sintering time increases to 45min, the densification degree of salt core is further improved, as shown in Fig. 9(c) and (f). This is because increasing the sintering time can increase the liquid phase volume, thereby enhancing the efficiency of particle rearrangement and mass transfer. However, the shrinkage will be generated during the solidification of the liquid phase, resulting in some closed pores in the salt core, most of which are spherical or nearly spherical.

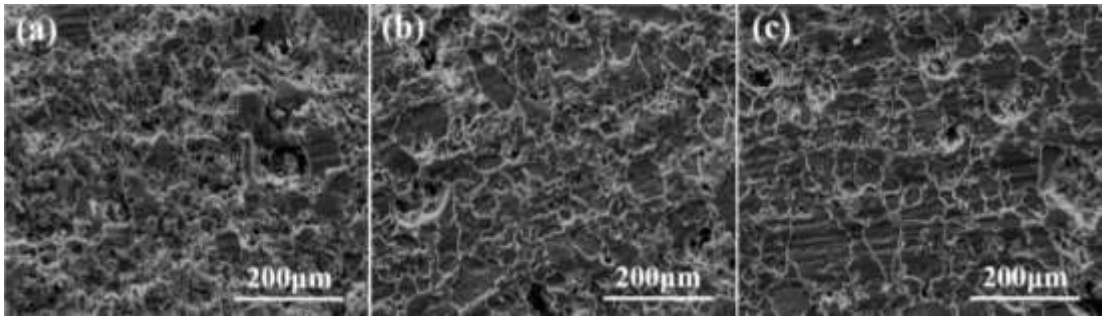

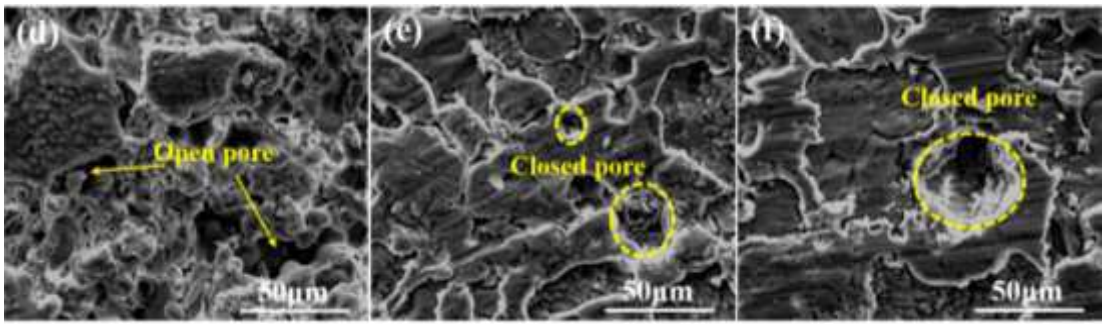

Fig. 9 Microstructures of salt core samples with 20 wt.% bauxite powder at different sintering time: (a, d) 15 min; (b, e) 30 min; (c, f) 45 min.

Generally, ceramic powder as a reinforcing material can improve the solidification structure of the salt cores [16,29]. The microstructures of the salt core samples with different bauxite powder contents at 30 min sintering are shown in Fig. 10, and Table 3 lists the EDS results of the salt cores selected in Fig. 10. According to the results of EDS analysis, it suggests that the components of the salt core are NaCl, Na_2SO_4 and bauxite powder, which matches the results of XRD and EDS maps analyses. It can be seen from Fig. 10 (a-d) that the NaCl phase is significantly refined with the increase of bauxite powder content, and the NaCl phase changes from coarse lath crystals to fine bulk crystals gradually. The grain refinement can promote the strength of the salt core, which can be explained by the Hall-Petch Eq. (6) [30], where σ represents the yield strength of the salt cores, D represents the mean grain size, σ_0 is the intrinsic yield strength and K is the material constant.

$$\sigma = \sigma_0 + KD^{-1/2} \quad (6)$$

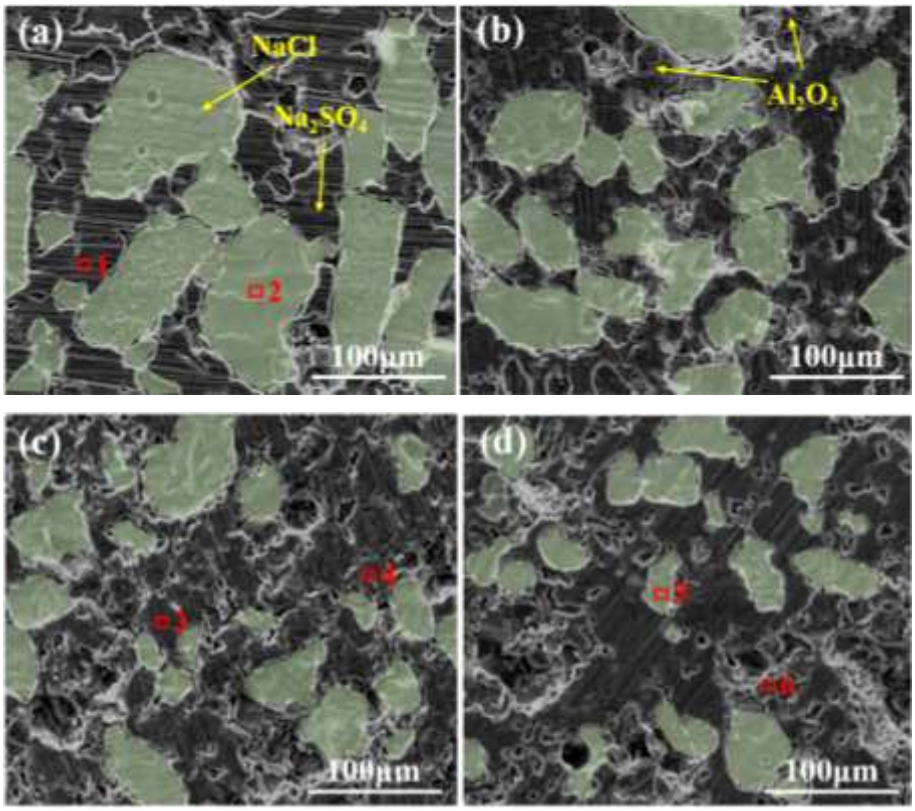

Fig. 10 Microstructures of salt core samples with different bauxite powder contents sintered for 30 min: (a) 0 wt.%; (b) 10 wt.%; (c) 20 wt.%; (d) 30 wt.%.

Table 3 EDS results of the selected positions of the salt core samples corresponding to Fig. 10.

Area no.	Element compositions (at.%)					component
	O	Na	Al	S	Cl	
1	36.37	32.93	-	30.7	-	Na_2SO_4
2	-	47.16	-	-	52.84	NaCl
3	37.63	33.74	-	28.63	-	Na_2SO_4
4	52.54	-	47.46	-	-	Al_2O_3
5	-	46.41	-	-	53.59	NaCl
6	58.78	-	41.22	-	-	Al_2O_3

The appropriate ceramic powder can improve the performance of the salt core, but excessive addition may have the opposite effect [29,31]. Many defects were observed when the bauxite powder content is 30 wt.%, as shown in Fig. 11, resulting in a decrease in the bending strength of the salt core.

Fig. 12 depicts the images of the salt core samples with 20 wt.% bauxite powder

under different sintering time. The side profile of the salt core samples are displayed in Fig. 12(a-d), and the cross-section profile of the salt core samples are displayed in Fig. 12(e-h). It is clear that the deformation degree of salt core increases with prolonging the sintering time. When the sintering time is 45 min, the salt core has a serious bending deformation, as shown in Figure 12 (d and h). Therefore, the sintering time of 30 min is the relatively optimal parameter.

The complex salt core samples were prepared using the optimized parameters, and the bauxite powder content and sintering time are 20 wt.% and 30 min, respectively, as shown in Fig. 13. It can be seen that the salt core samples after sintering have no obvious deformation, and no other defects are presented, indicating that it is feasible to manufacture a complex high-strength water-soluble salt core via LEF technology.

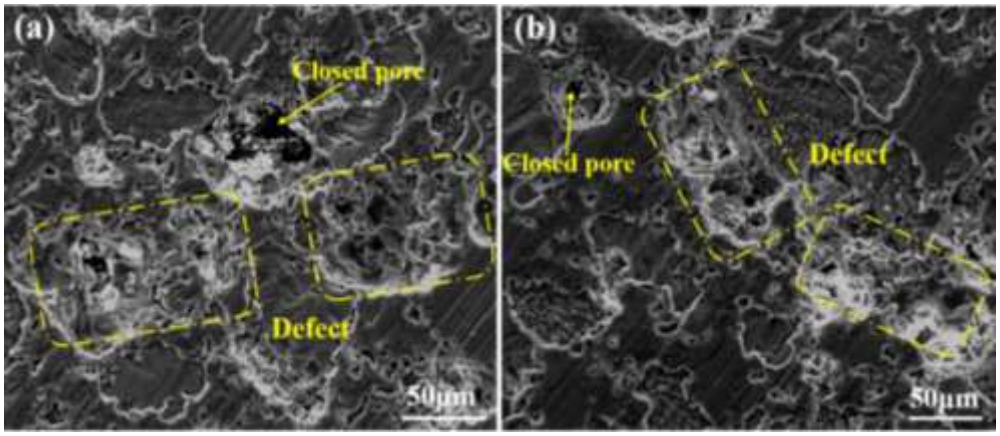

Fig. 11 Microstructures of salt core samples with 30 wt.% bauxite powder at different sintering time: (a) 30 min; (b) 45 min.

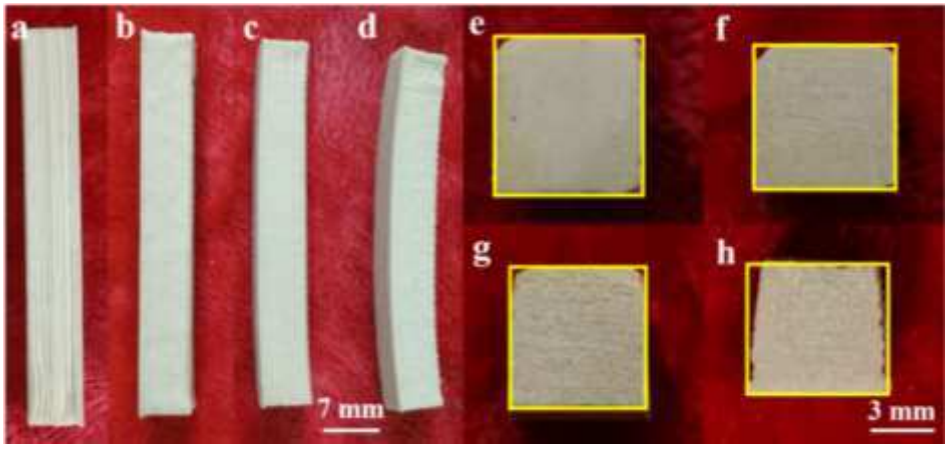

Fig. 12 Images of the salt core samples with 20 wt.% bauxite powder under different sintering time: (a, e) 0 min (green body); (b, f) 15 min; (c, g) 30 min; (d, h) 45min.

Fig. 13 Images of complex salt core samples fabricated by layered extrusion forming with the optimal parameters.

4 Conclusion

In this paper, we utilized the layered extrusion forming (LEF) method to prepare water-soluble salt cores strengthening by bauxite powder. The bauxite powder content and sintering parameters have a significant effect on the performance of the salt cores. Increasing the content of bauxite powder is beneficial to refine the NaCl phase, and prolonging the sintering time facilitates the densification of the salt core. However, excessive bauxite powder and longtime sintering are not conducive to the formation of the salt cores. The salt cores with 20 wt.% bauxite powder sintered for 30 min at 630℃ possess an excellent comprehensive performance, which satisfies the requirements for manufacturing hollow composite structure castings. The complex water-soluble high-strength salt core samples with high strength and well-shaped morphology are successfully fabricated under the optimal parameters, indicating the LEF is promising in the preparation of water-soluble salt cores.

Author contributions Xiaolong Gong, Xinwang Liu designed and participated in experiments, wrote the manuscript draft. Zheng Chen, Zhiyuan Yang performed the

experiments. Wenming Jiang analyzed the data. Zitian Fan directed this study, revised the manuscript and provided the funding. All the authors read and approved the final manuscript.

Funding The authors would like to thank the support of the National Nature Science Foundation of China (No.51775204 and 51971099), and the Analytical and Testing Center, HUST.

Availability of data and materials The data used to support the findings of this study are included within the article.

Declarations

Ethical approval Not applicable

Consent to participate Not applicable

Consent to publish Not applicable

Competing interests The authors declare no competing interests.

References

[1] Dong X, Yang H, Zhu X, Ji S (2019) High strength and ductility aluminium alloy processed by high pressure die casting. J Alloy Compd 773:86-96.

[2] Benedyk JC (2010) Aluminum alloys for lightweight automotive structures. USA: Illinois Institute of Technology Press.

[3] Alam T, Ansari AH (2017) Review on aluminium and its alloys for automotive applications. Int J Adv Technol Eng Sci 5:278-294.

[4] Wang T, Zha J, Jia Q, Chen Y (2016) Application of low-melting alloy in the fixture for machining aeronautical thin-walled component. Int J Adv Manuf Tech 87:2797-2807.

[5] Luo AA, Sachdev AK, Powell BR (2010) Advanced casting technologies for lightweight automotive applications. China Foundry 7:463-469.

[6] Kallien L, Weidler T, Becker M (2014) Production of magnesium die castings with hollow structures using gas injection technology in the hot chamber die casting process. Int Foundry Res 66:05-07.

[7] Jiang P, Liu FC, Fan ZT, Jiang WM, Liu XW (2016) Performance of water-soluble composite sulfate sand core for magnesium alloy castings. Arch Civ Mech Eng 14:494-502.

[8] Stauder BJ, Kerber H, Schumacher P (2016) Foundry sand core property assessment by 3-point bending test evaluation. J Mater Process Tech 237:188-196.

[9] Liu FC, Yang L, Huang Y, Jiang P, Li G, Jiang WM, Fan ZT (2017) Performance of resin bonded sand for magnesium alloy casting. J Manuf Process 30:313-319.

[10] Cho GH, Li J, Kim EH, Jung YG (2015) Preparation of a ceramic core with high strength using an inorganic precursor and the gel-casting method. Surf Coat Tech 284:396-399.

[11] Ke R, Dong Y (2021) Preparation and properties of water-soluble ceramic core for light alloy investment casting. Mater Today Commun 26:101918.

[12] Xiao Z, Harper LT, Kennedy AR, Warrior NA (2017) A water-soluble core material for

manufacturing hollow composite sections. Compos Struct 182:380-390.
[13] Yaokawa J, Miura D, Anzai K, Yamada Y, Yoshii H (2007) Strength of salt core composed of alkali carbonate and alkali chloride mixtures made by casting technique. Mater Trans 48:1034-1041.
[14] Beňo J, Adámková E, Mikšovský F, Jelínek P (2015) Development of composite salt cores for foundry applications. Mater Tehnol 49:619-623.
[15] Jiang W, Dong J, Lou L, Liu M, Hu Z (2010) Preparation and properties of a novel water soluble core material. J Mater Sci Techno 26:270-275.
[16] Liu FC, Tu S, Gong XL, Li GJ, Fan ZT (2020) Comparative study on performance and microstructure of composite water-soluble salt core material for manufacturing hollow zinc alloy castings. Mater Chem Phys 252:123257.
[17] Gong XL, Jiang WM, Liu FC, Yang ZY, Guan F, Fan ZT (2021) Effects of glass fiber size and content on microstructures and properties of KNO_3-based water-soluble salt core for high pressure die casting. Int J Metalcast 15:520-529.
[18] Jelínek P, Adámková E (2014) Lost cores for high-pressure die casting. Arch Foundry Eng 14:101-104.
[19] Sakoda T, Suzuki T (1976) Water soluble core for pressure die casting and process for making the same. US3963818A.
[20] Compton BG, Lewis JA (2015) 3D-printing of lightweight cellular composites. Adv Mater 26:5930-5935.
[21] Tang SY, Yang L, Li GJ, Liu XW, Fan ZT (2019) 3D printing of highly-loaded slurries via layered extrusion forming: Parameters optimization and control. Addit Manu 28:546-553.
[22] Li GJ, Tang SY, Yang L, Qian L, Jiang WM, Fan ZT (2019) Fabrication of soluble salt-based support for suspended ceramic structure by layered extrusion forming method. Mater Design 183:108173.
[23] Tang SY, Fan ZT, Zhao HP, Yang L, Liu FC, Liu XW (2018) Layered extrusion forming—a simple and green method for rapid prototyping ceramic core. Int J Adv Manuf Tech 96:3809-3819.
[24] Zhang YM, Shao HP, Lin T, Peng J, Wang AY, Zhang ZN, Wang LH (2019) Effect of Ca/P ratios on porous calcium phosphate salt bioceramic scaffolds for bone engineering by 3D gel-printing method. Ceram Int 45:20493-20500.
[25] Kleger N, Cihova M, Masania K, Studart AR, Lffler JF (2019) 3D printing of salt as a template for magnesium with structured porosity. Adv Mater 31:1903783.
[26] Jakus AE, Geisendorfer NR, Lewis PL, Shah RN (2018) 3D-Printing Porosity: A new approach to creating elevated porosity materials and structures. Acta Biomater 72:94-109.
[27] Qian L, Yang L, Li G, Jiang WM, Fan ZT (2020) Effect of nano-TiO_2 on properties of 3 mol% yttria-stabilized zirconia ceramic via layered extrusion forming. J Eur Ceram Soc 40:4539-4546.
[28]https://www.crct.polymtl.ca/fact/phase_diagram.php?file=NaCl-Na2SO4.jpg&dir=FTsalt.Accessed 16 May 2020.
[29] Tu S, Liu FC, Li GJ, Jiang WM, Liu XW, Fan ZT (2018) Fabrication and characterization of high-strength water-soluble composite salt core for zinc alloy die castings. Int J Adv Manuf Tech 95:505–512.
[30] Zhang HJ, Sun SL, Hiu HJ, Zhu Z, Wang YL (2020) Characteristic and mechanism of nugget performance evolution with rotation speed for high-rotation-speed friction stir welded 6061 aluminum alloy. J Manuf Process 60:544-552.
[31] Huang R, Zhang B (2017) Study on the composition and properties of salt cores for zinc alloy die

424 casting. Inter J Metalcast 11:440–447.
425

Figures

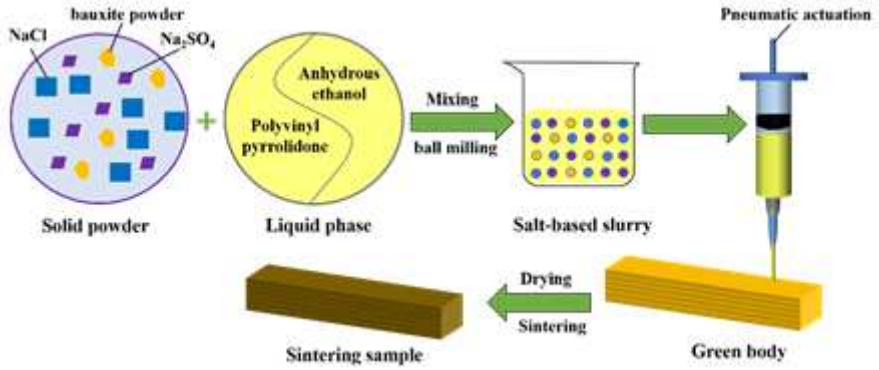

Figure 1

Schematic diagram of the LEF technology to prepare water-soluble salt cores.

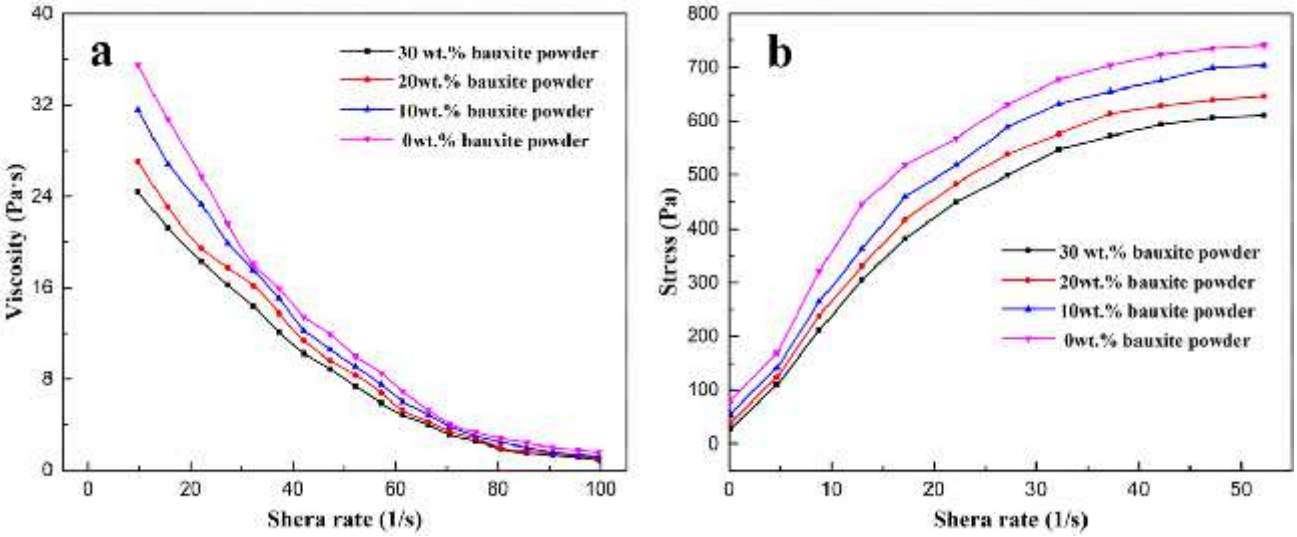

Figure 2

Rheological behaviors of salt-based slurry with different bauxite powder contents: (a) viscosity versus shear rate and (b) stress versus shear rate.

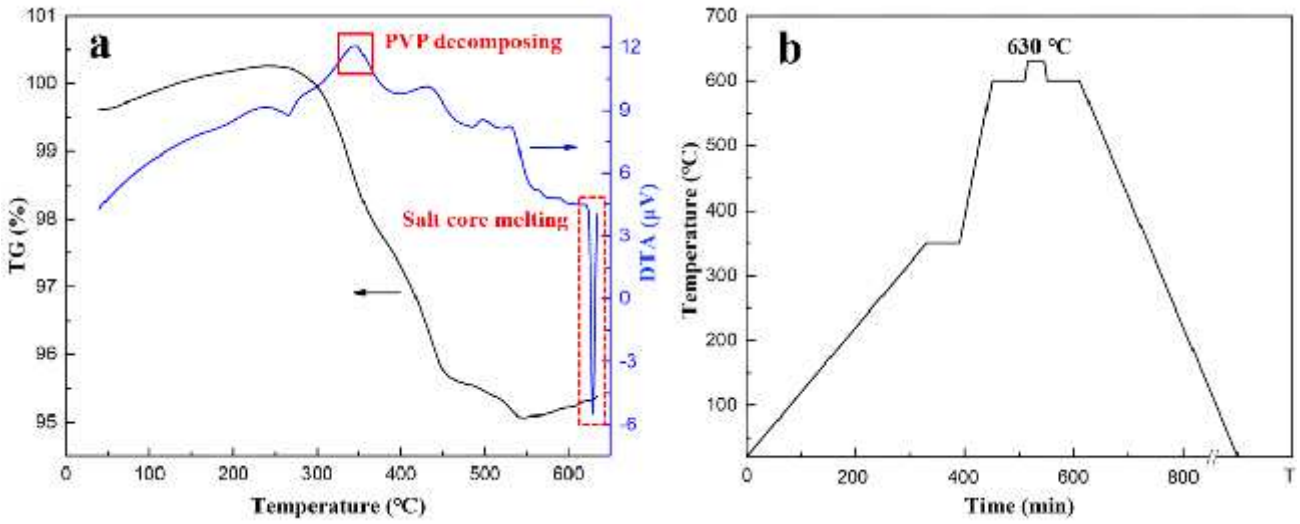

Figure 3

Sintering process of salt core green body: (a) TG-DTA curves and (b) sintering temperature versus sintering time.

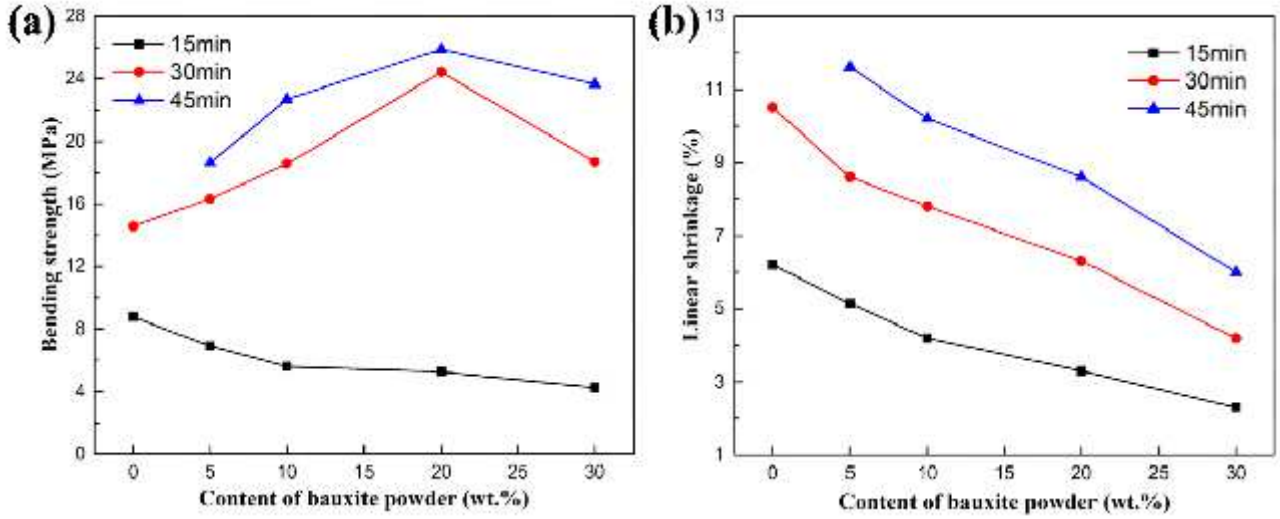

Figure 4

Effects of bauxite powder content at various sintering time on the salt core samples: (a) bending strength and (b) linear shrinkage.

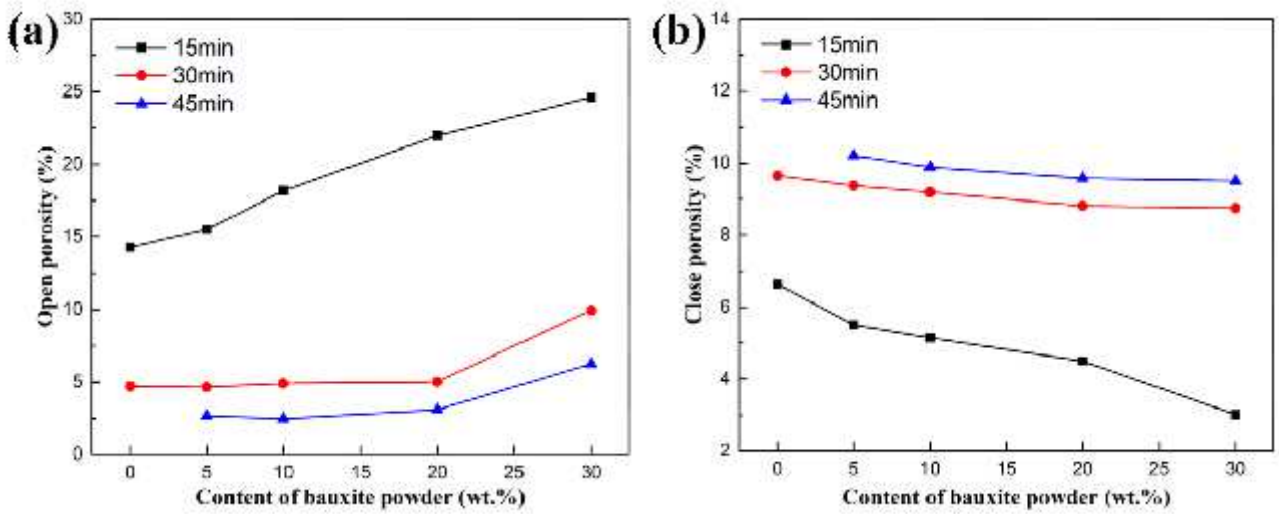

Figure 5

Effects of bauxite powder content at various sintering time on the salt core samples: (a) open porosity and (b) close porosity.

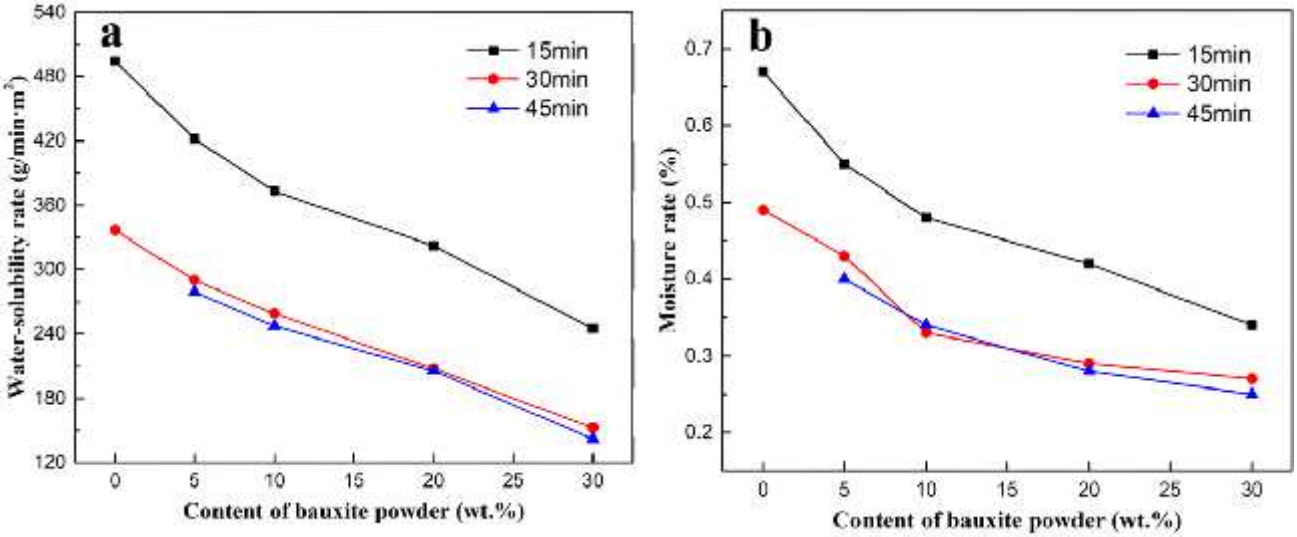

Figure 6

Effects of bauxite powder content at various sintering time on the salt core samples: (a) water-solubility rate and (b) moisture rate.

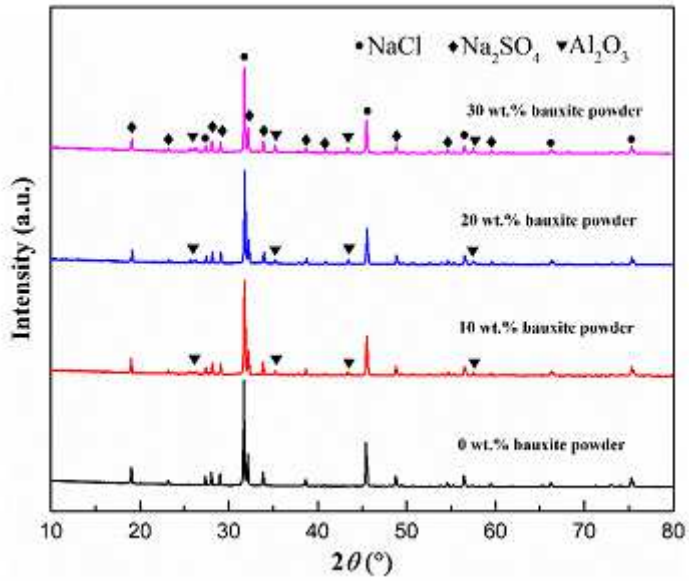

Figure 7

XRD pattern of the salt core with different bauxite powder contents sintered for 30 min.

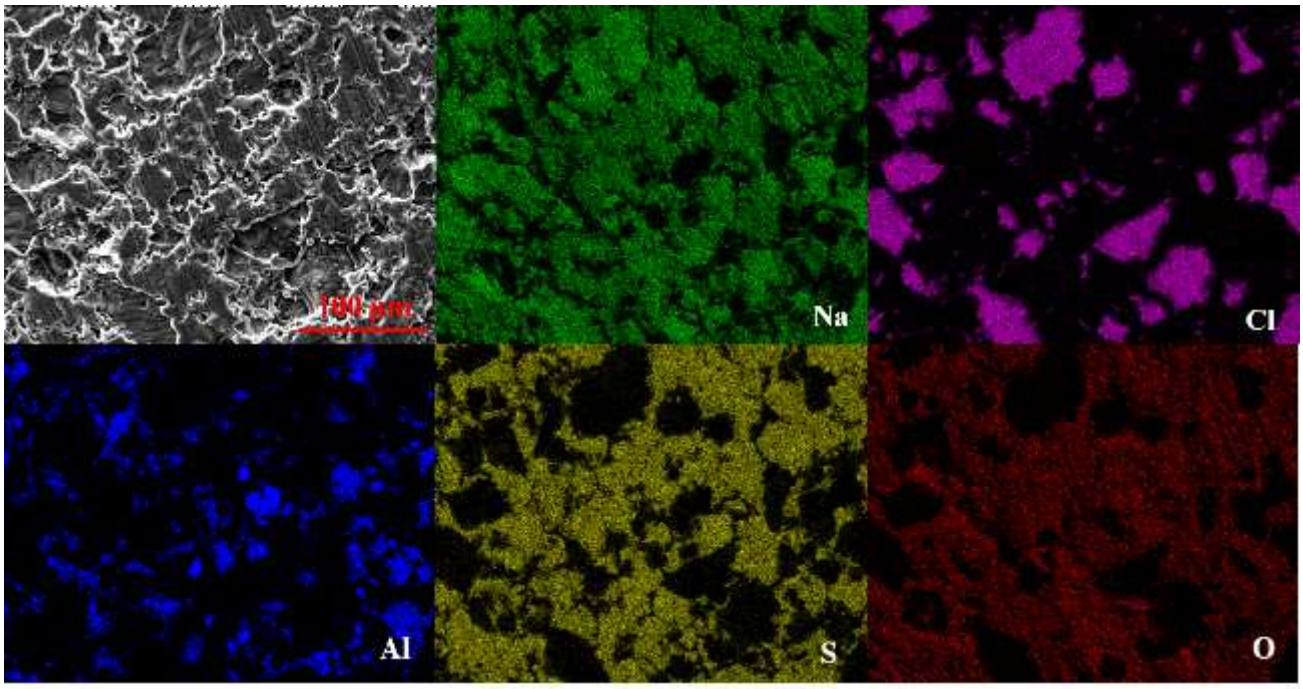

Figure 8

EDS maps analyses of salt core samples with 20 wt.% bauxite powder sintered for 30 min.

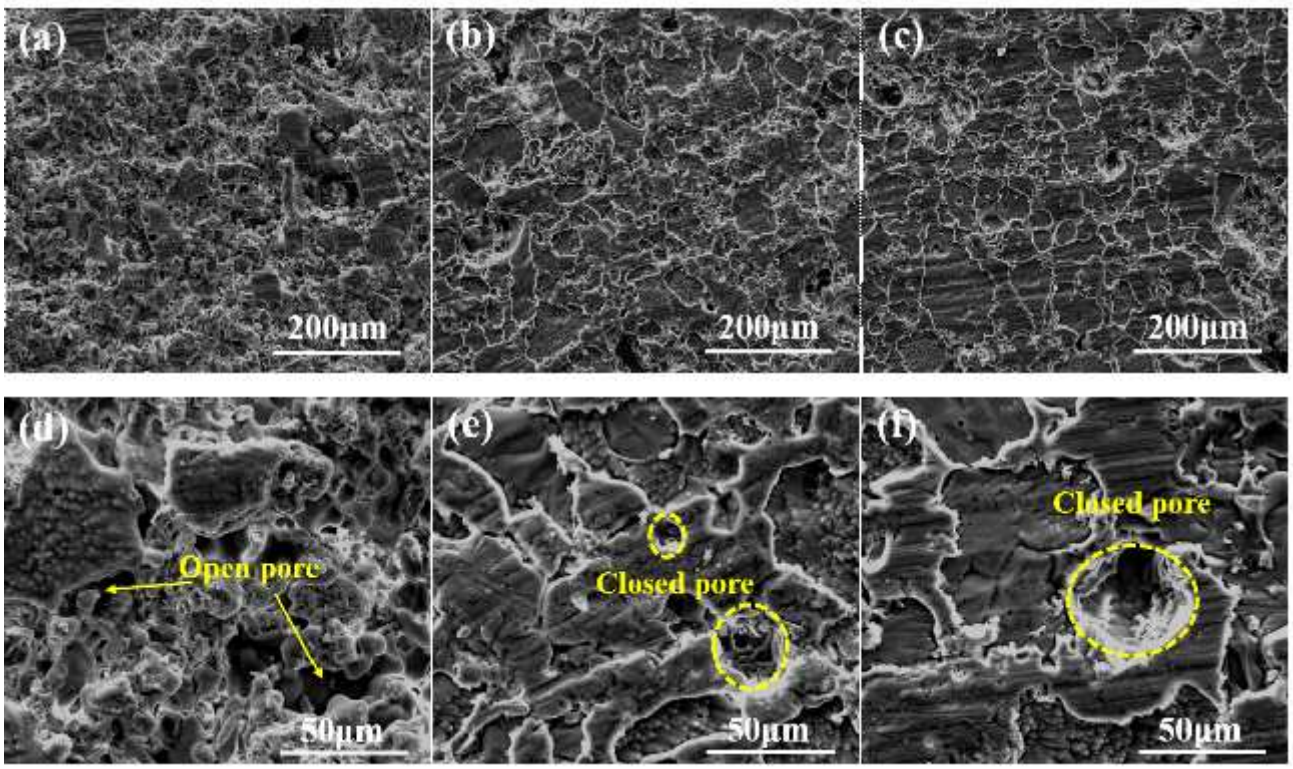

Figure 9

Microstructures of salt core samples with 20 wt.% bauxite powder at different sintering time: (a, d) 15 min; (b, e) 30 min; (c, f) 45 min.

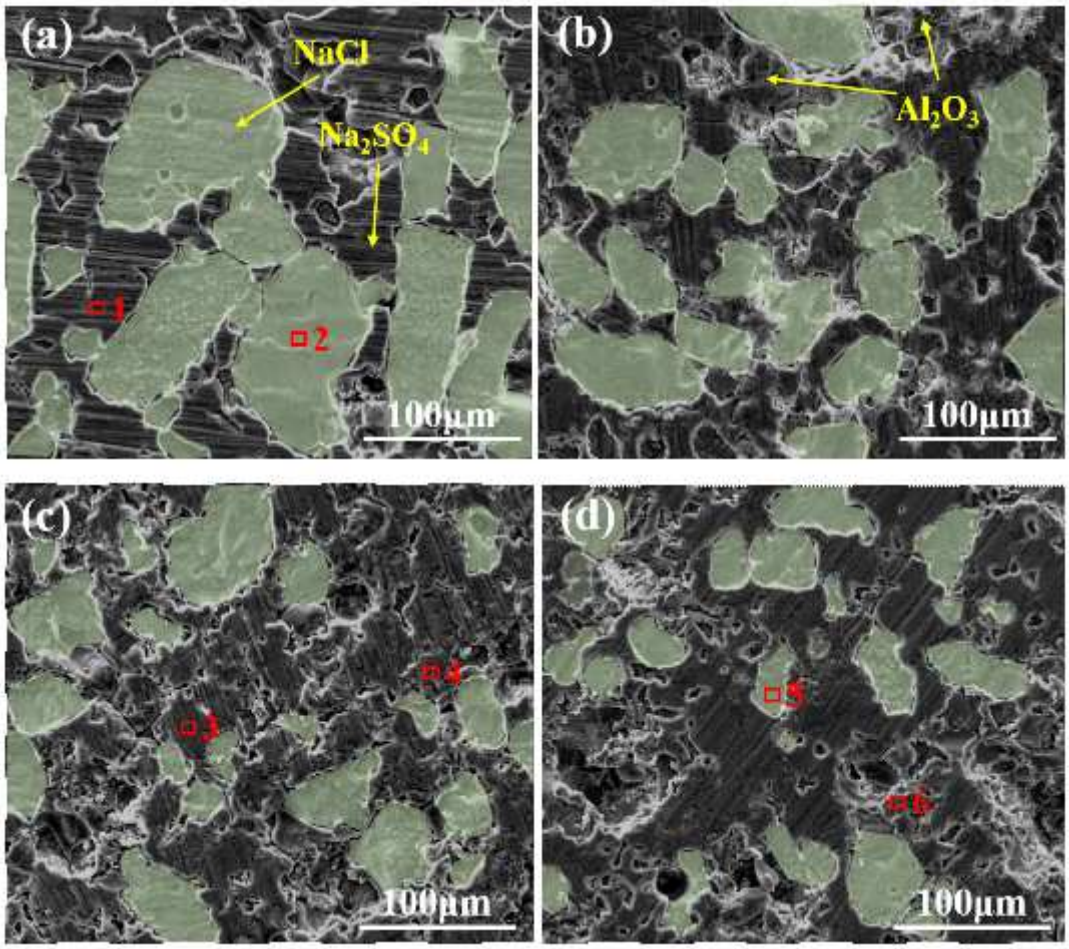

Figure 10

Microstructures of salt core samples with different bauxite powder contents sintered for 30 min: (a) 0 wt.%; (b) 10 wt.%; (c) 20 wt.%; (d) 30 wt.%.

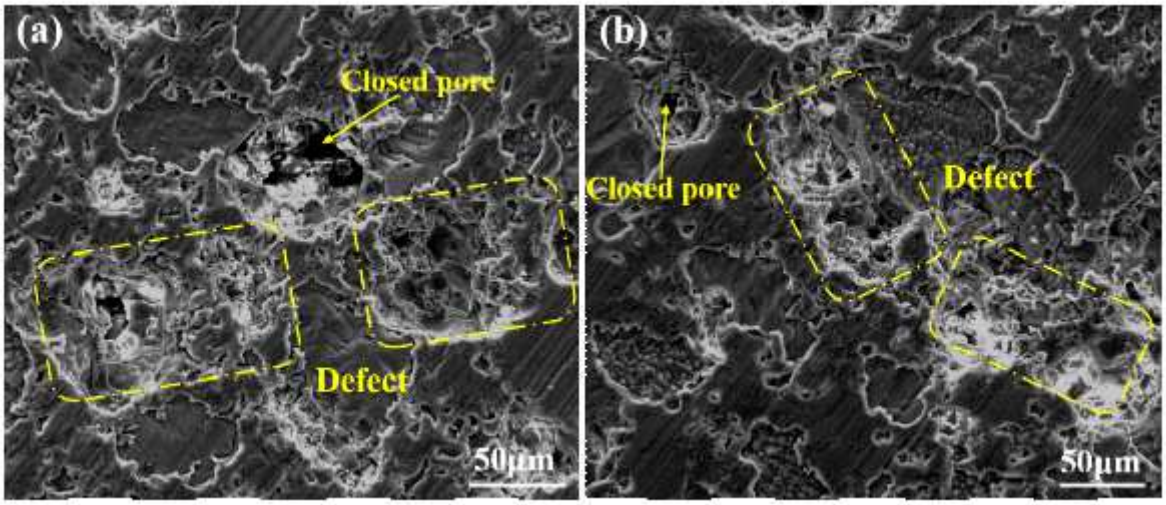

Figure 11

Microstructures of salt core samples with 30 wt.% bauxite powder at different sintering time: (a) 30 min; (b) 45 min.

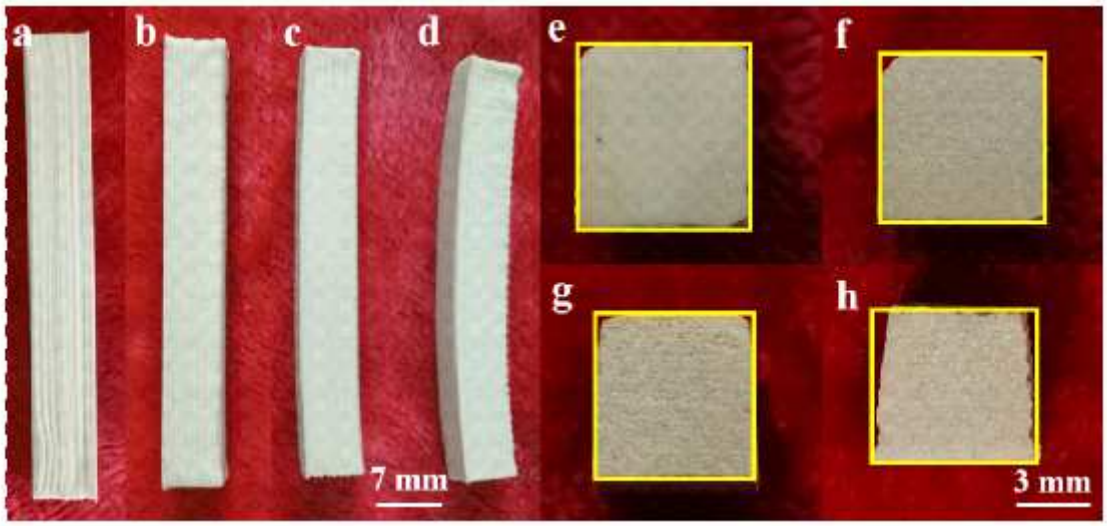

Figure 12

Images of the salt core samples with 20 wt.% bauxite powder under different sintering time: (a, e) 0 min (green body); (b, f) 15 min; (c, g) 30 min; (d, h) 45min.

Figure 13

Images of complex salt core samples fabricated by layered extrusion forming with the optimal parameters.